JOURNAL OF OPTOELECTRONICS AND ADVANCED MATERIALS, Vol. 10, No. 11, November 2008, p. 2932 - 2935

Microstructure of magnetite doped elastomers investigated by SAXS and SANS

M. BALASOIU[a,c*], M. L. CRAUS[b,c], A. I. KUKLIN[c], J. PLESTIL[d], V. HARAMUS[e], A. H. ISLAMOV[c], R. ERHAN[a,c], E. M. ANITAS[f,c], M. LOZOVAN[b], V. TRIPADUS[a], C. PETRESCU[f], D. SAVU[g], S. SAVU[g], I. BICA[g]

[a]*National Institute of Physics and Nuclear Engineering, Bucharest*
[b]*National Institute of Research and Development for Technical Physics, Iasi, Romania*
[c]*Joint Institute of Nuclear Research, Dubna, Russia*
[d]*Institute of Macromolecular Chemistry, Academy of Sciences of the Czech Republic, Prague*
[e]*GKSS Forschungszentrum, Geesthacht, Germany*
[f]*ICPE SA Bucharest, Romania*
[g]*West University of Timisoara, Department of Electricity and Magnetism, Timisoara, Romania*

We present some recent results on the SAXS and SANS investigations of the magnetic elastomers. Samples were obtained by polymerizing dimethylsiloxane with Fe_3O_4 ferrofluid in a magnetic field and without magnetic field and characterized by XRD, SANS and SAXS. The SAXS maximum at large angles, obtained from magnetic elastomers, was fitted by using a Pseudo-Voigt function. It was found that the Fe_3O_4 particles lead to a significant change of the local structure of elastomer, meaning the decrease of the quasi-crystalline phase and the micro-strains into the matrix. The average particle size obtained from SANS measurements agrees well with the average particle size determined by XRD and SAXS analysis. The splitting of the SANS intensity owing to an additional scattering in zero field reflects the existence of magnetic correlations inside the Q region of 0.005 $Å^{-1}$< Q < 0.02 $Å^{-1}$.

(Received September 1, 2008; accepted October 30, 2008)

Keywords: SANS, SAXS, Magnetic elastomers, Ferrofluids, Fe_3O_4, XRD, Local structure

1. Introduction

Magnetic elastomers belong to a specific class of so-called smart materials because they can respond to changes in their environment. They are composed of magnetic particles and a low-permeability matrix. Applying an external magnetic field, a structure will be formed inside the material or the structure embedded in the material will be changed.

Combination of magnetic and elastic properties leads to different phenomena which are exhibited in a variable magnetic field [1-3]. It opens new possibilities for technological applications as (i) magnetoelastic composite with particles made of magnetostrictive hard or soft ferromagnetic material [4, 5]; (ii) magnetorheological elastomers for application in airplane and car industries as actuators or anti-friction components [6]; (iii) heat-shrinkable elastic ferromagnets with variable magnetic and conductive properties [7].

Other applications that utilize magnetic polymer nanocomposites are currently emerging at a high rate. Examples include magnetic actuation in microelectromechanical systems (MEMS) and medical devices, thermal actuation through electromagnetic power harvesting, and magnetically actuated morphing structures [8].

Such composites are quite new and understanding of the behavior of these materials depending on the composition, external conditions, and the synthesis processes is intensively under investigation [9].

The magnetoelastic properties of composites are not the bare sum of the elasticity of the polymer and the stiffness and magnetic properties of the filler, but are the result of a complex synergy of several effects, referring to different length scales and detectable by different techniques.

Many studies of the observed reinforcing effect from magnetic fillers have approached the problem from a magneto-mechanical point of view and investigated the microscopic properties through the study of the magneto-elastic responses of the composite [1-3,10]. Less well understood, however, is the effect of the polymer-filled interaction with the local distribution of polymer around filler on a submicroscopic length scale.

Work making use of scattering techniques as neutron and X-rays is more rare but if used, is based on the scattering vector dependence or exploit the full advantage relating the intensity to the volume of the scattering particle [11,12].

2. Experimental

The studied samples, obtained at the Department of Electricity and Magnetism, West University of Timisoara [13-15], are composed from oil based 7.7% particle volume

concentration Fe_3O_4 ferrofluid [16] with oleic acid as surfactant, embedded in a polymer matrix formed from dimethylsiloxane, dibutyltindilaurate benzyl silicate, polymerized in zero field (sample A) or in an applied magnetic field of H=108,28 kA/m (sample B).

In order to determine the phase composition, lattice micro-distortions and average size of coherent length (average size of mosaic blocks) the samples were investigated by XRD. The XRD measurements were performed using DRON diffractometer, CoKα radiation. XRD data were handled using Ceck Cell and Rietveld software.

The samples were studied using small angle X-ray (SAXS) and neutron (SANS) scattering methods. SAXS experiments were performed at Rigaku spectrometer, using a pinhole camera (Molecular Metrology SAXS System) attached to a microfocused X-ray beam generator (Osmic MicroMax 002). The camera was equipped with a multiwire, gas-filled area detector with an active area diameter of 20 cm (s. a schematic representation of small angle diffraction setup in Fig.1). Two experimental setups were used to cover the *Q* range of 0.007 -1.1 $Å^{-1}$ (Fig.3).

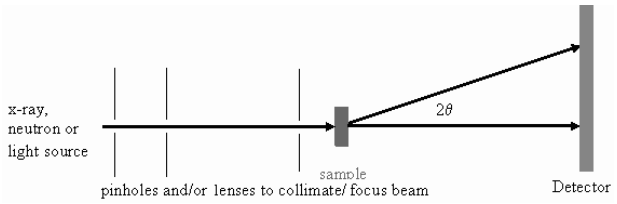

Fig. 1. Schematic representation of small angle diffraction setup.

The SANS experiments were carried out on the YUMO diffractometer [17] at the IBR-2 pulsed reactor, JINR, Dubna and on SANS-1 [18] installed at Geesthacht Germany in the Q-range of about 0.003-0.3 $Å^{-1}$.

3. Small angle scattering elements

In the small angle neutron scattering experiment, $d\Sigma(Q)/d\Omega$, the differential scattering cross section is measured as a function of the momentum transfer, $Q = (4\pi / \lambda) \sin(\Theta/2)$. λ is the neutron's wavelength and Θ - the scattering angle.

Typically, scattering experiments at a given value of Q probe a length scale D, where D is the dimension of the inhomogeneities producing the scattering.

$$D = 2\pi/Q \qquad (1)$$

The SANS range is usually defined by $0 < Q < \pi/D$. For dilute systems of randomly oriented particles (neglecting size polydispersity) in the region of small Q values ($QR_g<1.2$), Guinier's law is applied and the scattering is given by the relation:

$$d\Sigma(Q)/d\Omega = d\Sigma(0)/d\Omega \exp(-R_g^2 Q^2/3) \qquad (2)$$

where $d\Sigma(0)/d\Omega$ is the scattering at zero angle and R_g is the radius of gyration of the particle i.e., the root-mean-square distance of all scattering elements from the centre of gravity. If this approximation holds, the plot ln I(Q) versus Q^2 should show a linear dependence in the region of small Q. The characteristic size of a particulate system can be easily obtained within this approximation. For instance, for spherical particles, one can relate the radius of particle R with the radius of gyration by $R = (5/3)^{1/2} R_g$ [19].

4. Discussions

From XRD data results that the elastomer was doped with Fe_3O_4 particles about 10 nm average size, the elastomers contain practically the same concentration of Fe_3O_4, but with different average size of coherent blocks and microstrains.

The data were handles with PowderCell, to obtain the lattice constants, average size of crystalline blocks and microstrains. It was established that both samples contain a small amount of foreign phase (s. Fig.2).

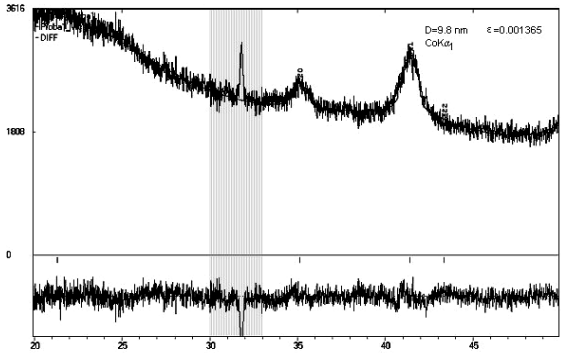

Fig.2. Observed and calculated difractograms (upper-side); difference between observed and calculated difractograms (bottom-side) for Fe_3O_4 particles.

To obtain exact lattice constant, the average size of mosaic blocks and microstrains of magnetite we used a Rietveld program. In agreement with the literature data, magnetite crystallizes in GS 227, with a=8.38 Å; atomic position in unit cell are given in Table 1.

Table 1 Atomic position (x, y, z), occupation and temperature factor (B)

Ion	Atomic coordinates			Occupation	B
	x	y	z		
Fe^{3+}	0.125	0.125	0.125	1.0	0.25
Fe^{3+}	0.500	0.500	0.500	0.5	0.35
Fe^{2+}	0.500	0.500	0.500	0.5	0.35
O^{2-}	1.000	1.000	0.754	1.0	1.32

Data concerning SAXS measurements indicated a strong difference of the structure of doped and undoped with Fe_3O_4 particles samples. We had observed the systematic appearance of a Bragg diffraction peak in SAXS plots in the large region of Q values (near Q=0.9Å^{-1}; see in Fig.3). The lattice parameter of quasi-crystal was obtained by fitting the observed maximum with a Pseudo-Voigt profile function (see Fig.4).

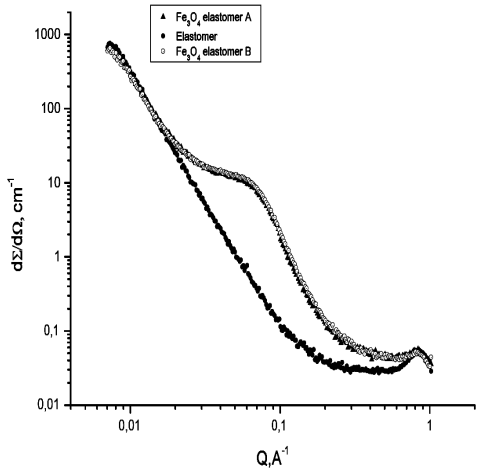

Fig. 3. SAXS experimental curves from sample A, B and simple elastomer obtained at Rigaku spectrometer in function at IMC, Prague.

We suppose that the elastomer is fragmented into small particles ordered. Doping with Fe_3O_4 particles leads to a significant change of the local structure of elastomer, meaning the decrease of the quasi-crystalline phase concentration (s. Fig.3) and the average size of the crystalline blocks (see Table 2).

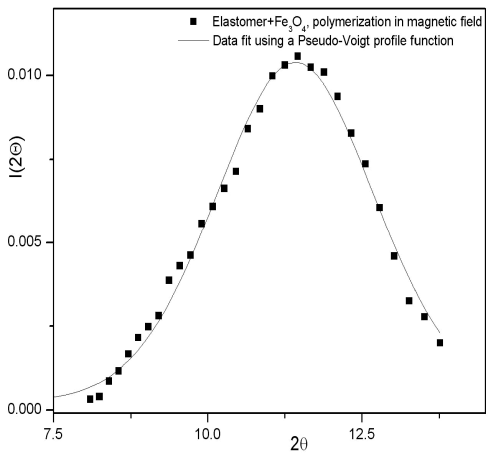

Fig. 4. Fit of the XRD data using a Pseudo-Voigt profile function.

The average size of elastomer blocks (Δ) decreases, while the ordering distance (D) increases, when a magnetic field is applied during the polymerization process (s. Table 2).

Fig. 5 shows the curves of the neutron scattering cross section for the samples of the Fe_3O_4 elastomer polymerized in zero magnetic field (sample A) and in a magnetic field of H=108,28 kA/m (sample B).

Following the data evaluation of [9] we use the fact that in the case of the sample B polymerized in magnetic field, the magnetization of most of the particles is aligned in the direction of the applied field. In this case, the forced common magnetic alignment extends to such large distances that it can not be resolved any more by SANS.

The scattering then originates from nanometer sized particles surrounded by particle boundaries of different (nuclear and magnetic) density.

Table 2.Variation of gravity center (θ), average size of crystalline blocks (Δ) and ordering distance (D) into the elastomer matrix.

Sample	θ	Δ (nm)	D (nm)
Elastomer matrix	11.56±0.02	2.73±0.04	0.77±0.001
Elastomer with Fe_3O_4 particles (polymerization without magnetic field)	11.71±0.01	2.38±0.13	0.77±0.001
Elastomer with Fe_3O_4 particles (polymerization with magnetic field)	11.41±0.05	2.73±0.14	0.77±0.01

The average particle size obtained from these measurements agrees well with the average particle size determined by XRD and SAXS analysis.

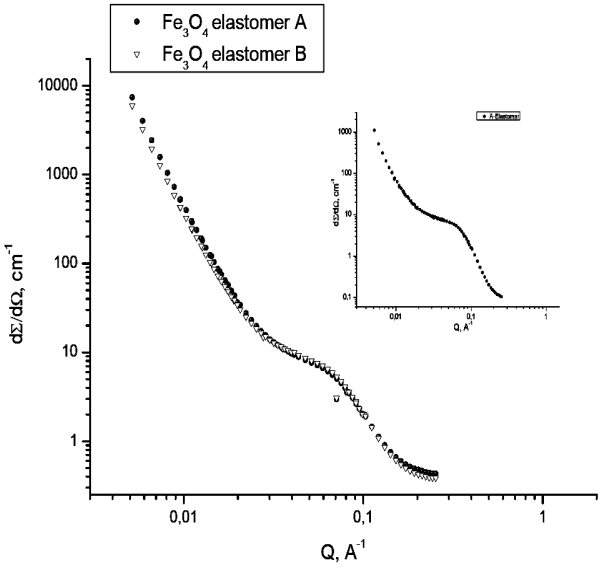

Fig. 5. SANS scattering from elastomer A (with scattering from pure elastomer substracted); SANS scattering from Elastomer A (scattering from pure elastomer extracted) (top image); curves obtained at SANS-1 in function at GeNF.

Table 3 Radius of gyration and particle radius ($R = (5/3)^{1/2} R_g$) obtained from SAXS and SANS measurements, respectively.

Sample	R_g/SAXS	R_g/SANS	R(nm)
Elastomer with Fe_3O_4 particles polymerization without magnetic field (A)	1.9±0.01	2.29±0.05	2.45±0.01 2.95±0.06
Elastomer with Fe_3O_4 particles polymerization with magnetic field (B)	2±0.01	2.3±0.05	2.58±0.01 2.96±0.06

The corresponding scattering curves of the neutron scattering cross section for the samples polymerized in zero magnetic field and in a magnetic field lie closely together and are parallel for large Q values; for smaller Q values a splitting is observed. The splitting of the SANS intensity owing to an additional scattering in zero field reflects the magnetic correlations inside the Q region of $0.005\ Å^{-1} < Q < 0.02\ Å^{-1}$ existence.

Such correlations were also found in other SANS studies [20-26].

5. Conclusions

It was obtained that: the profile of diffraction maximum belonging to magnetite can be fitted by using a Pseudo-Voigt function. We found that one type of magnetite particles are nanometer size (9.8 nm). The samples contain small amount of foreign phases (around $2\theta = 32^{\circ}$). We supposed that the elastomer is fragmented into small particle ordered at short distance. Doping with Fe_3O_4 particles leads to a significant change of the local structure of elastomer, meaning the decrease of the micro-strains into the matrix.

The average magnetite particle size obtained from SANS measurements agrees well with the average particle size determined by XRD and SAXS analysis.

The corresponding scattering curves of the neutron scattering cross section for the samples polymerized in zero magnetic field and in a magnetic field lie closely together and are parallel for large Q values; for smaller Q values a splitting is observed. The splitting of the SANS intensity owing to an additional scattering in zero field reflects the existence of magnetic correlations inside the Q region of $0.005\ Å^{-1} < Q < 0.02\ Å^{-1}$. This shows that the magnetic correlations are not confined to single particles, but extend across the interfaces and result in a common, localized magnetic alignment of many grains.

In future we intend to perform, systematic investigations concerning structure, magnetic and elastic properties of elastomers doped with magnetic nanoparticles.

Acknowledgements. The grants of Romanian Governmental Plenipotentiary at JINR are acknowledge

References

[1] Yu. L. Raikher, O. V. Stolbov, Magneto-deforming effect in ferroelastane, Letter to JTF **26**(4), 47 (2000) (Rus.)

[2] L. Lanotte, et al., J. Optoelectron. Adv. Mater. **6**(2), 523 (2004).

[3] S. Abramchuk, E. Kramarenko , G. Stepanov, L. V. Nikitin, G. Filipcsei, A. R. Khokhlov, M. Zrínyi, Polymers for Advanced Technologies **18**(11), 883 (2007).

[4] A. Boczkowska, S. F. Awietjan, R. Wroblewski, Smart. Mater.Strut. **16**, 1924 (2007).

[5] G. Y. Zhou, Smart Mater. Struct. **12**, 139 (2003).

[6] G. Auerhammer, D. Collin, P. Martinoty, J. Chem.Phys. **124**, 204907-1-10 (2006).

[7] S. Peng, M. Zhang, X. Niu, W. Wen, P. Sheng, Appl. Phys. Lett. **92,** 012108-1-3 (2008).

[8] M. Farshad, Andre Benine, Polymer Testing, **23**(3), 347 (2004).

[9] E. M. Anitas, A. Kh. Islamov, M. Balasoiu, C. Muresan, I. Bica, Yu. S. Kovalev, O. L. Orelovich, A. I. Kuklin, J. Optoelectron. Adv. Mater. (2008) (accepted).

[10] S. Ahmed, J. Mater. Sci. **25**, 4933 (1990)

[11] A. Emmerling, P. Wang, G. Popp, A. Beck, J. Frike, J. Phys. **13**, 357 (1993).

[12] A. Botti, W. Pyckhout-Hintzen, V. Urban, J. Kohlbrecher, D. Richter, E. Straube, Appl. Phys. **A 74** (Suppl.) S513 (2002).

[13] I. Bica, J. Ind. Eng. Chem. **12**(5), 806 (2006).

[14] I. Bica, J. Magn. Magn. Mater. **241**, 196 (2002).

[15] I. Bica, J. Ind. Eng. Chem., **11**(2), 299 (2007).

[16] L. Vekas, CIMTEC, A-3 **IL01**, 11 (2008)

[17] A. I. Kuklin, A. Kh. Islamov, V. I. Gordely, Neutron News **16(**3), 16 (2005).

[18] H. B.Stuhrmann et al., Nucl. Instr. Meth. **A356**, 133 (1995).

[19] M. Balasoiu, B. Grabcev, D. Bica, Romanian Reports in Physics **47**(3-5), 319 (1995).

[20] W. Wagner, et al., J.Mater.Sci. **6**, 2305 (1991).

[21] W. Wagner, H. Van Swygenhoven, H. Hofler, A. Wiedenmann, Nanostructured Materials **6,** 929 (1995).

[22] J. F. Loffler, H. B. Braun, W. Wagner, Phys. Rev. Lett., **85**(9), 1990 (2000).

[23] J. Weissmuller et al., Mater. Res. Soc. Symp. Proc. **457**, 231(1998)

[24] V.L.Aksenov et al., Appl.Phys. Vol. A74 (Suppl.) (2002) S943-S944

[25] F. L. O. Paula, R. Aquino, G. J. da Silva, J. Depeyrot, F. A. Tourinho, J. O. Fossum, K. D. Knudsen, J. Appl. Cryst. **40,** s269 (2007).

[26] M. E. Dokukin, N. S. Perov, E. B. Dokukin, A. H. Islamov, A. I. Kuklin, Yu. E. Kalinin, A. V. Sitnikov, Iz. RAN, Seria Fizicheskaya, **71**(11) 1643 (2007).

*Corresponding author: balasoiumaria@yahoo.com